JOC*Article*

New Cytotoxic Salinosporamides from the Marine Actinomycete *Salinispora tropica*

Philip G. Williams, Greg O. Buchanan, Robert H. Feling, Christopher A. Kauffman, Paul R. Jensen, and William Fenical*

Center for Marine Biotechnology and Biomedicine, Scripps Institution of Oceanography, University of California−San Diego, La Jolla, California 92093-0204

wfenical@ucsd.edu

Salinosporamide B (**3**)　　　Salinosporamide C (**4**)
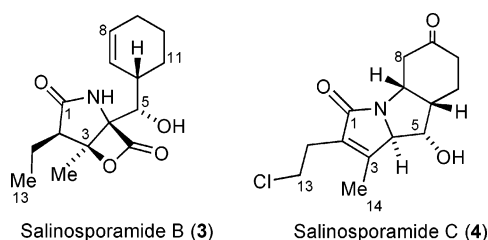
An extensive study of the secondary metabolites produced by the obligate marine actinomycete *Salinispora tropica* (strain CNB-392), the producing microbe of the potent proteasome inhibitor salinosporamide A (**1**), has led to the isolation of seven related γ-lactams. The most important of these compounds were salinosporamide B (**3**), which is the deschloro-analogue of **1**, and salinosporamide C (**4**), which is a decarboxylated pyrrole analogue. New SAR data for all eight compounds, derived from extensive testing against the human colon carcinoma HCT-116 and the 60-cell-line panel at the NCI, indicate that the chloroethyl moiety plays a major role in the enhanced activity of **1**.

Bacteria belonging to the order Actinomycetales (commonly called actinomycetes) are one of the most prolific resources for lead compounds in the development of new pharmaceuticals.[1] Unfortunately, after more then 50 years of intense scrutiny, the rate that new biologically active metabolites are being discovered from terrestrial actinomycetes has been steadily diminishing.[2] If these chemically prolific microorganisms are to continue to provide new structures that are of medicinal relevance, then new strategies that lead to the isolation of genetically novel strains must be found. Investigations targeting actinomycetes have traditionally focused on soil-derived strains,[3] but recent evidence has unequivocally shown that the marine environment is host to a wide range of taxonomically diverse actinomycetes.[4]

In 1991, we cultivated an unusual group of actinomycetes from marine sediments.[5] Further examination showed that this group was unique among the actinomycetes, as all members required seawater for growth. Phylogenetic characterization revealed that these strains represented a new genus for which the name "*Salinospora*" was originally proposed.[6] This name was subsequently changed to *Salinispora* in the formal taxonomic description.[7] Examination of more than 120 distinct *Salinispora* strains from the two currently recognized species *S. tropica* and *S. arenicola*[7] showed that greater than 80% of these organisms produced culture extracts that inhibited the in vitro growth of human colon carcinoma HCT-116.

Examination of the culture broth of *S. tropica* strain CNB-392 led to the isolation of salinosporamide A (**1**), which has an unusual fused γ-lactam-β-lactone ring structure.[8,9] Salinosporamide A (**1**) is structurally related to clasto-lactacystin β-lactone (**2**, omuralide),[10] a trans-

(1) Berdy, J. *J. Antibiot.* **2005**, *58*, 1−26.

(2) Bull, A. T.; Ward, A. C.; Goodfellow, M. *Microbiol. Mol. Bol. Rev.* **2000**, *64*, 573−604.

(3) Okami, Y.; Hotta, K. In *Actinomycetes in Biotechnology*; Goodfellow, M., Williams, S. T., Mordarski, M.; Academic Press: New York, 1988; pp 33−67.

(4) (a) Jensen, P. R.; Gontang, E.; Mafnas, C.; Mincer, T. J.; Fenical, W. *Environ. Microbiol.* **2005**, *7*, 1039−1048. (b) Maldonado, L. A.; Stach, J. E. M.; Pathom-aree, W.; Ward, A. C.; Bull, A. T.; Goodfellow, M. *Antonie van Leeuwenhoek* **2005**, *87*, 11−18. (c) Montalvo, N. F.; Mohamed, N. M.; Enticknap, J. J.; Hill, R. T. *Antonie van Leeuwenhoek* **2005**, *87*, 27−36.

(5) Jensen, P. R.; Dwight, R.; Fenical, W. *Appl. Environ. Microbiol.* **1991**, *57*, 1102−1108.

(6) Mincer, T. J.; Jensen, P. R.; Kauffman, C. A.; Fenical, W. *Appl. Environ. Microbiol.* **2002**, *68*, 5005−5011.

(7) Maldonado, L. A.; Fenical, W.; Jensen, P. R.; Kauffman, C. A.; Mincer, T. J.; Ward, A. C.; Bull, A. T.; Goodfellow, M. *Int. J. Syst. Evol. Micr.*, published on-line April 15, 2005.

formation product of the microbial metabolite lactacystin.[11] Compounds **1** and **2** are unique because they specifically inhibit the proteolytic activity of the 20S subunit of the proteasome without affecting any other protease activity. The proteasome is a multicatalytic complex that regulates intracellular protein degradation through three distinct proteolytic activities (chymotrypsin-like, trypsin-like, and caspase-like).[12] One protein that is regulated by the proteasome is the transcription factor NF-κB.[12] This transcription factor promotes cell survival by regulating genes encoding cell-adhesion molecules, proinflammatory cytokines, and antiapoptotic proteins.[13] NF-κB is constitutively active in many malignancies, including multiple myeloma (MM), and interfering with its activity through the use of proteasome inhibitors is the basis of the FDA-approved antitumor drug Velcade.[14] Interestingly, salinosporamide A is not only a nanomolar inhibitor of the 20S subunit of the proteasome but also active against Velcade-resistant multiple myeloma cells.[15] This combination of potent biological activity and structural novelty has attracted considerable interest in the synthetic community, which has culminated in the synthesis of **1**[16] and **2**.[17] It has also prompted a closer examination of the extract of the culture broth of *S. tropica* strain CNB-392. We report

(8) Feling, R. H.; Buchanan, G. O.; Mincer, T. J.; Kauffman, C. A.; Jensen, P. R.; Fenical, W. *Angew. Chem., Int. Ed.* **2003**, *42*, 355−357.

(9) Recently, compounds analogous to **1** that lacked the chlorine substituent were reported from a terrestrial actinomycete of the genus *Streptomyces*. Stadler, M.; Seip, S.; Mueller, H.; Mayer-Bartschmid, A.; Bruening, M.-A.; Benet-Buchholz, J.; Togame, H.; Dodo, R.; Reinemer, P.; Bacon, K.; Fuchikami, K.; Matsukawa, S.; Urbahns, K. U.S. Patent 2004071382, 2004.

(10) (a) Dick, L. R.; Cruikshank, A. A.; Grenier, L.; Melandri, F. D.; Nunes, S. L.; Stein, R. L. *J. Biol. Chem.* **1996**, *271*, 7273−7276. (b) Corey, E. J.; Li, W.-D. Z. *Chem. Pharm. Bull.* **1999**, *47*, 1−10 and references therein.

(11) Omura, S.; Fujimoto, T.; Otoguro, K.; Matsuzaki, K.; Moriguchi, R.; Tanaka, H.; Sasaki, Y. *J. Antibiot.* **1991**, *44*, 113−116 and references therein.

(12) Adams, J. *Proteasome Inhibitors in Cancer Therapy*. Humana Press: Totowa, New Jersey, 2004.

(13) Wang, C. Y.; Mayo, M. W.; Korneluk, R. G.; Goeddel, D. V.; Baldwin, A. S., Jr. *Science* **1998**, *281*, 1680−1683.

(14) Richardson, P. G.; Barogie, B.; Berenson, J.; Singhal, S.; Jagannath, S.; Irwin, D.; Rajkumar, S. V.; Srkalovic, G.; Alsina, M.; Alexanian, R.; Siegel, D.; Orlowski, R. Z.; Kuter, D.; Limentani, S. A.; Lee, S.; Hideshima, T.; Esseltine, D. L.; Kauffman, M.; Adams, J.; Schenkein, D. P.; Anderson, K. C. *N. Engl. J. Med.* **2003**, *348*, 2609−2617.

(15) Chauhan, D.; Catley, L.; Li, G.; Podar, K.; Hideshima, T.; Mitsiades, C.; Ovaa, H.; Berkers, C.; Munshi, N.; Chao, T.; Nicholson, B.; Neuteboom, S. T.; Richardson, P.; Palladino, M.; Anderson, K. C. *Cancer Cell*, submitted.

(16) (a) Reddy, L. R.; Saravanan, P.; Corey, E. J. *J. Am. Chem. Soc.* **2004**, *126*, 6230−6231. (b) Endo, A.; Danishefsky, S. J. *J. Am. Chem. Soc.* **2005**, *127*, 8298−8299. (c) Reddy, L. R.; Fournier, J.-F.; Reddy, B. V. S.; Corey, E. J. *Org. Lett.* **2005**, *7*, 2699−2701.

(17) (a) Crane, S. N.; Corey, E. J. *Org. Lett.* **2001**, *3*, 1395−1397. (b) Corey, E. J.; Reichard, G. A.; Kania, R. *Tetrahedron Lett.* **1993**, *34*, 6977−80. (c) Nagamitsu, T.; Sunazuka, T.; Tanaka, H.; Omura, S.; Sprengeler, P. A.; Smith, A. B., III *J. Am. Chem. Soc.* **1996**, *118*, 3584−90. (d) Corey, E. J.; Li, W.; Reichard, G. A. *J. Am. Chem. Soc.* **1998**, *120*, 2230−2236. (e) Corey, E. J.; Li, W.; Nagamitsu, T. *Angew. Chem., Int. Ed.* **1998**, *37*, 1676−1679. (f) Corey, E. J.; Li, W. *Tetrahedron Lett.* **1998**, *39*, 8043−8046. (g) Corey, E. J.; Li, W. *Chem. Pharm. Bull.* **1999**, *47*, 1−10. (h) Panek, J. S.; Masse, C. E *Angew. Chem., Int. Ed.* **1999**, *38*, 1093−1095. (i) Soucy, F.; Grenier, L.; Behnke, M. L.; Destree, A. T.; McCormack, T. A.; Adams, J.; Plamondon, L. *J. Am. Chem. Soc.* **1999**, *121*, 9967−9976. (j) Crane, S. N.; Corey, E. J. *J. Org. Chem.* **2003**, *68*, 2760−2764. (k) Brennan, C. J.; Pattenden, G.; Rescourio, G. *Tetrahedron Lett.* **2003**, *44*, 8757−8760. (l) Ooi, H.; Ishibashi, N.; Iwabuchi, Y.; Ishihara, J.; Hatakeyama, S. *J. Org. Chem.* **2004**, *69*, 7765−7768. (m) Corey, E. J.; Li, W. *Tetrahedron Lett.* **1998**, *39*, 7475−7478. (n) Reddy, L. R.; Saravanan, P.; Fournier, J.-F.; Reddy, B. V. S.; Corey, E. J. *Org. Lett.* **2005**, *7*, 2703−2705.

TABLE 1. NMR Spectral Data for 1 and 3 at 300 MHz

C/H	**1** δ_H^a multiplicity (J in Hz)	**1** δ_C^b	**3** δ_H^a multiplicity (J in Hz)	**3** δ_C^b
1		176.4, C		176.9, C
2	3.17, t (7.1)	46.2, CH	2.72, dd (8.8, 5.8)	49.8, CH
3		86.1, C		86.3, C
4		80.2, C		79.3, C
5	4.24, d (9.2)	70.9, CH	4.24, t (8.8)	70.4, CH
6	2.85, br m	39.2, CH	2.90, m	38.7, CH
7	6.42, d (10.1)	128.4, CH	6.44, d (10.3)	128.2, CH
8	5.88, m	128.8, CH	5.88, m	128.4, CH
9	1.91, m	25.3, CH$_2$	1.92, m	24.7, CH$_2$
10a 10b	1.38, m 1.66, m	21.7, CH$_2$	1.39, m 1.72, m	21.1, CH$_2$
11a 11b	1.66, m 2.37, m	26.5, CH$_2$	1.72, m 2.32, m	25.9, CH$_2$
12a 12b	2.32, m 2.48, m	29.0, CH$_2$	1.90, m 2.14, m	18.5, CH$_2$
13a 13b	4.01, m 4.14, m	43.2, CH$_2$	1.21, t (7.3)	12.3, CH$_2$
14	2.07, s	20.0, CH$_3$	2.05, s	20.2, CH$_3$
15		169.0, C		169.1, C
NH	10.60, br s		10.42, br s	
OH	7.60, br s		7.49, d (8.8)	

a Recorded in C$_5$D$_5$N. *b* Number of attached protons determined by DEPT experiments.

here the results of that study which has led to the isolation of salinosporamide B (**3**) and C (**4**), along with five other related compounds, and the evaluation of their biological activities.

Salinosporamide A (**1**)   Omuralide (**2**)   Salinosporamide B (**3**)   Salinosporamide C (**4**)

5   6   7

8   9
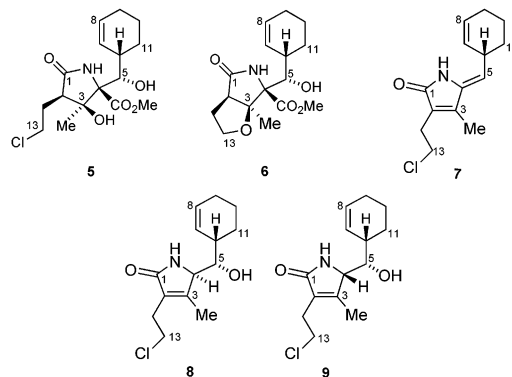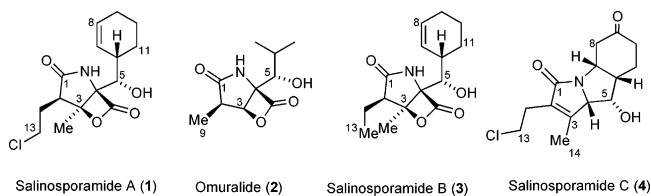
Salinosporamide B (**3**), which was obtained from ethyl acetate as amorphous crystals, was the second most abundant component in the culture extract. High-resolution mass spectral analysis suggested a molecular formula of C$_{15}$H$_{20}$NO$_4$, which was in accord with the structural information provided by the ^{13}C NMR spectrum (Table 1). The IR data of **3** exhibited absorptions at 1700 and 1820 cm^{-1} indicative of amide and β-lactone functionalities, respectively, suggesting that **3** was a structural analogue of **1**. This was supported by the ^{1}H

NMR spectrum of **3** that displayed most of the diagnostic resonances present in **1**, including an isolated methyl group (δ_H 2.05, s), a *cis*-alkene (δ_H 6.44, d and 5.88, m), and an amide proton signal (δ_H 10.42, br s). There were noticeable differences, though, in the ^{1}H NMR spectrum of **3**, which included an upfield shift of the H-12 methylene proton signal and the presence of a methyl triplet (δ_H 1.21, t). All this information, including differences in the molecular formulae for **1** and **3**, suggested that **3** was an analogue of **1** that lacked the chlorine substituent. This was confirmed by analysis of the gCOSY and gHMQC data (Table S1, Supporting Information) which revealed all the spin systems in **3** and established the planar structure of **3** as 13-deschlorosalinosporamide A. The relative stereochemistry of **3** was determined to be identical to that of **1** on the basis of analysis of the NOESY spectral data and the proton−proton coupling constants. Specifically, enhancements between H-14 and H-5 and from H-14 to H-2 established their syn relationship and thus the relative stereochemistry around the bicyclic ring, while the similarity of the proton−proton coupling constant between H-5 and H-6 (**1**; $^3J_{5H,6H}$ = 9.2, **2**; $^3J_{5H,6H}$ = 8.8) suggests the same configuration at these centers. Finally, since the literature[18] suggests that the replacement of a halide by a hydrogen atom, if it is distant from a chiral center, has only a small effect (10−20%) on the magnitude of the optical rotation, and since both **1** and **3** are levorotatory {**1**; $[\alpha]_D^{25}$ −72.9° (*c* 0.55, MeOH); **2** $[\alpha]_D^{25}$ −54.5° (*c* 0.286, MeOH)}, the latter has been assigned the same absolute configuration (2*R*,3*S*,4*R*,5*S*,6*S*) as was determined by X-ray analysis of **1**.[8,19,20]

Examination of the other HPLC fractions led to the isolation of a more polar compound salinosporamide C (**4**). The elemental composition of this compound, as determined by HRMALDI−FTMS, was $C_{14}H_{19}ClNO_3$ on the basis of the observance of a pseudomolecular ion peak at 284.1059 (MH⁺, +0.6 mDa). While this molecular formula required the same number of degrees of unsaturation (6) that was required by the elemental composition of **1**, it was clear from the other spectral data (Table 2) that the structural features of **1** and **4** differed significantly.

Analysis of the ^{13}C NMR spectrum of **4**, recorded in pyridine-d_5, allowed all of the degrees of unsaturation to be assigned to an amide (δ_C 176.9), a ketone (δ_C 210.1),

(18) Jacque, J.; Gros, C.; Mourcier, S. *Absolute Configurations of 6000 Selected Compounds with One Asymmetric Carbon Atom*; Georg Thieme Publishers: Stuttgart, Germany, 1997. Specifically, see references for data on 1-chloro-4-methylhex-1-en-3-one, 1-chloro-4-methylhexane, 1-chloro-5-methylheptane, 1-bromo-3-methylnonane, 1-bromo-4-methylnonane, and the corresponding deshalogenated compounds.

(19) All of our attempts to convert **1** into **3** resulted in cleavage of the β-lactone and subsequent decarboxylation. Dechlorination of **1** was attempted using (a) Mg in *i*-PrOH with sonication for 4 days; (b) hydrogenation with 10% Pd/C in *i*-PrOH; and (c) NaBH₄ reduction in *i*-PrOH and also in DMSO. An attempt was also made to convert **1** to the iodo derivative using the Finkelstein reaction (NaI in refluxing acetone), which under these conditions was not successful.

(20) It should be noted that the structural representation of **1** used in this manuscript is different than that used in the original paper[8] where the structure was originally disclosed. During the review process on this manuscript, it was brought to our attention that the original figure was in violation of the IUPAC rules because a hashed line between two adjacent stereocenters (C-4 and C-5) is not allowed under this system. The stereochemical representations used in this paper for **1**−**9** are in accord with these IUPAC recommendations. See: Moss, G. P. *Pure Appl. Chem.* **1996**, *68*, 2193−2222.

TABLE 2. NMR Spectral Data for 4 at 300 MHz

C/H	$\delta_H{}^a$ multiplicity (*J* in Hz)	$\delta_C{}^{b,c}$	COSY	HMBC^{d,e}	ROESY
1		176.9, C		4, 7, 12, 14	
2		128.5, C		4, 12, 13, 14	
3		157.2, C		4, 12, 14	
4	4.23, d (8.2)	71.4, CH	5, 14	5, 6, 7, 14	10a, 14
5	4.05, br t (8.2)	74.4, CH	OH, 4, 6	4, 6, 7	6, 11b
6	2.85, m	45.8, CH	7, 11		
7	4.41, dt (6.4, 5.9)	53.7, CH	6, 8	8, 11	5, 6, 8a, 8b
8a	3.00, m	45.5, CH₂	7, 8b		
8b	2.89, m		7, 8a		
9		210.1, C		7, 8, 10, 11	
10a	2.57, m	38.5, CH₂	10b, 11b	6, 8, 11	
10b	2.34, m		10a		
11a	2.35, m	20.5, CH₂	11b	5, 6, 7, 10	
11b	2.12, m		10a, 11a		
12	2.72, m	27.8, CH₂	13	13, 14	
13	3.83, m	43.6, CH₂	12	12	12
14	2.09, br s	13.1, CH₃	4		
OH	7.47, br d		5		

a Recorded in C_5D_5N. *b* Recorded at 100 MHz. *c* Number of attached protons determined from an edited HSQC spectrum. *d* Protons showing long-range correlation with indicated carbon. *e* Correlations were observed for $^nJ_{CH}$ = 8 Hz.
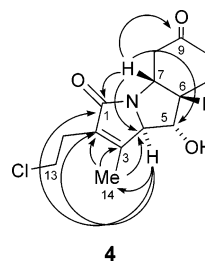
FIGURE 1. Key HMBC correlations used to establish the structure of **4**.

a carbon−carbon double bond (δ_C 157.2, 128.5), and, by elimination, three rings. On the basis of the chemical shifts of the olefinic carbons, it was clear that this carbon−carbon double bond was in conjugation with either the ketone or the amide carbonyl. The former was the case, as HMBC correlations from an allylic methyl proton signal at δ_H 2.09 (H-14) and a methylene signal at δ_H 2.72 (H-12) to C-1, C-2, and C-3 established the amide carbonyl as part of an α,β-unsaturated system (C-1 through C-3) (Figure 1). The second carbonyl (C-9) was assigned as part of a substituted cyclohexanone ring (C-6 through C-11) on the basis of a network of COSY and HMBC correlations (Table 2), which could be extended at C-6 to include two downfield methine signals (δ_H 4.05 and 4.23) on the basis of COSY correlations between H-6/H-5 and H-5/H-4. This substructure was then joined to the α,β-unsaturated amide on the basis of HMBC correlations between H-4 and C-3 to form a tricyclic system containing all the carbons (Figure 1). The final ring connectivities were established by HMBC correlations, specifically from H-7 and H-4 to the amide carbonyl (C-1) and between H-7 and C-4, to give the hexahydro-3*H*-pyrrolo-[1,2*a*]-indol-3,6-dione ring structure depicted.

The relative stereochemistry of **4** was established by a two-dimensional ROESY NMR experiment (Figure 2). A ROESY correlation between H-7 and H-6 established a *cis* junction in the cyclohexanone ring, while ROESY correlations between H-7 and H-5 and H-5 and H-6

FIGURE 2. ROESY correlations used to establish the relative configuration of **4**.

FIGURE 3. NOESY correlations used to establish the relative configuration of **6**.

established the configuration of the proton at H-5. Finally, ROESY cross-peaks between H-4 and H-10a established the rest of the relative stereochemistry.

LC-MS analysis of the extract from the large-scale fermentation of this *S. tropica* strain identified five more minor analogues of **1** that were subsequently isolated to provide compounds **5**−**9**. These compounds were produced in comparable yields to salinosporamide B (**3**) and C (**4**), but only in trace amounts when compared to **1**. The structures of these compounds were deduced as follows (See Tables S2−S6 in Supporting Information for tabulated spectral data). The ^{1}H NMR spectrum of compound **5** was essentially identical to that of **1**, except that it contained an additional methyl resonance at δ_H 3.69. This suggested that **5** was the methyl ester analogue of the seco-acid of **1**. This conclusion was consistent with both the molecular formula of $C_{16}H_{24}ClNO_5$, which was determined by HRMS analysis in conjunction with the NMR data (See Tables S2 and S3). Compound **6** also possessed a methoxy singlet in its ^{1}H NMR spectrum. This resonance again suggested that the β-lactone ring of **1** had been opened to the methyl ester, but the molecular formula of **6** ($C_{16}H_{24}NO_5$) still required the same number of rings as in **1**. The other important conclusion that was clear from the molecular formula of **6** was that this derivative did not incorporate chlorine. Comprehensive analysis of the two-dimensional NMR data, recorded in CDCl$_3$ (Table S4), allowed the gross structure of **6** to be assigned. Specifically, the cyclohexene ring was established on the basis of HMBC correlations from the vinyl protons H-7 and H-8 to the carbons of this ring (H-7 to C-5, C-6, C-8, C-9, and C-11; H-8 to C-6, C-7, C-9, and C-10), while HMBC correlations from H-2 and H-14 to C-1, C3, and C-4 established the presence of the β-lactam ring functionality. Finally, HMBC correlations from H-2 to C-12 and C-13 indicated that the two-carbon side chain of **1** was still intact but revealed that the chemical shift of C-13 in **6** was significantly further downfield than the corresponding carbon signal in **1**. This, in conjunction with HMBC correlations from H-13a and H-13b to C-3, established that **6** was a tetrahydrofuran analogue of **1**. The relative configuration of the β-lactam ring in **6** was established on the basis of interpretation of the NOESY NMR data. Cross-peaks were observed from H-2 to H-14 and between H-14 and H-5, indicating that these three protons were in a syn orientation around the β-lactam ring (Figure 3). The relative configuration of the vicinal centers C-5 and C-6
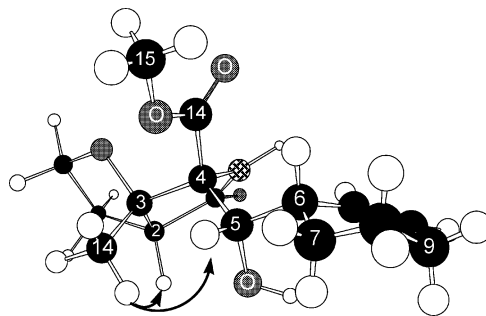
was assigned as 5R*,6R* on the basis of comparison of the $^3J_{H,H}$ values (in pyridine-d_5) between these centers in **1**, **5**, and **6** (See Tables 1 and S2).

The molecular formula of **7** was established as $C_{14}H_{18}$-ClNO by HRMALDI−FTMS, indicating that **7** contained six double-bond equivalents. Some of these degrees of unsaturation were reflected in the UV chromophore of **7**, which showed a significant bathochromic shift as compared to **1** and **3**. This suggested extended conjugation, which was also reflected in the IR spectrum of **7**, which showed an infrared carbonyl absorption at a lower wavenumber (1684 cm^{-1}) than seen in the other compounds. Analysis of the proton and carbon NMR data indicated that **7** was structurally related to **1**. For example, the NMR data clearly showed that the chloroethyl and cyclohexene moieties were present in **7** on the basis of the characteristic proton resonances for H-12, H-7, and H-8 (δ_H 3.55, 5.66, and 5.48), but it also revealed some differences. Specifically, the NMR data indicated the presence of additional trisubstituted (δ_H 4.89; δ_c 114.7, CH; δ_c 138.2, C) and tetrasubstituted alkenes (δ_c 128.4, C; δ_c 143.3, C) as well as the loss of the signal for the proton adjacent to the amide carbonyl (H-2). These data, in conjunction with the rest of the NMR information (Tables S2 and S3) established the structure of **7** as the α,β,γ,δ-unsaturated lactam shown. The geometry of the exocyclic double bond in **7** was assigned as *Z* on the basis of an NOE correlation between the vinyl methine proton and the methyl signal at C-14.

Compound **8** was isolated as a colorless oil. The HRMALDI−FTMS data defined the molecular formula of **8** as $C_{14}H_{20}ClNO_2$, which was 44 amu less than salinosporamide A (**1**). This difference was reflected in the ^{13}C NMR spectrum of **8** in which only 14 resonances were observed (Table S3). The most prominent difference, as compared to **1**, was the absence of the ester carbonyl signal at δ_C 169.0, which implied that the β-lactone moiety was not present in **8**. In contrast, the β-lactam ring structure was present in **8**, as suggested by HMBC correlations (Table S5) from the allylic methyl proton signal (H-14) to C-1, C-2, C-3, and C-4. Interestingly, C-4, which had been a quaternary carbon in **1,3** and **5**−**7**, now showed a $^1J_{CH}$ to a proton signal at δ_H 3.70, which was coupled to the amide proton signal at δ_H 8.55. This signal at δ_H 3.70 also displayed a COSY correlation to the oxygenated methine proton signal at 3.27 ppm. This in turn could be connected to the cyclohexene ring on the basis of a series of COSY and HMBC correlations (See Table S5). These signals defined the α,β-unsaturated γ-lactam structure of **8**.
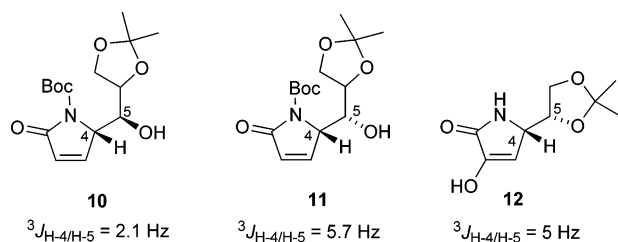
FIGURE 4. Model compounds used to establish the relative configuration of **8** and **9**.

The low-resolution mass spectral data for compounds **8** and **9** showed that they were isomers, since both gave the same pseudomolecular ion at 270.1 (MH$^+$), which corresponded to the molecular formula $C_{14}H_{20}ClNO_2$, which was determined by HRMS. Analysis of the two-dimensional NMR data established that **9** (Table S6) had the same planar structure as **8** (Table S5), indicating that they were not constitutional isomers. A detailed comparison of the ^{1}H NMR spectra for the two compounds revealed that they were configurational isomers. This was based on the multiplicity of the H-4 proton signal; in compound **8**, H-4 was a broad singlet when the proton NMR spectrum was recorded in C_6D_6, while in **9** this signal was a doublet. Of the possible sites of epimerization that would explain this difference in the multiplicity of the H-4 proton signal, C-4 and C-5, the former is more likely based on mechanistic considerations (vide infra). While the relative configurations of **8** and **9** were not rigorously established, a tentative assignment for C-4/C-5 was postulated on the basis of comparison of the proton–proton coupling constants between H-4 and H-5 of **8** and **9** with that of model compounds recorded in the appropriate solvent. Comparison of the literature coupling constants between H-4 and H-5[21] for the anti and syn diastereomers of the model compounds **10** and **11** suggest that the latter has the larger $^3J_{4H,5H}$ value (2.1 vs 5.7 Hz respectively; CDCl$_3$). A 5 Hz proton–proton coupling constant was also observed in the related compound **12** that also has a syn configuration at these two stereogenic centers (Figure 4).[22] This suggests that the C-4/C-5 junction is *anti* in **8** ($^3J_{H-4/H-5}$ 1.3 Hz) and *syn* in **9** ($^3J_{H-4/H-5}$ = 6.7 Hz, CDCl$_3$; the rest of the data in this solvent are not shown).

The presence of the methyl esters in **5** and **6** raises suspicion that these compounds were artifacts of the isolation procedure and not produced in the fermentation process. To test this hypothesis, **1** (1.8 mg) was stirred in a 1:1 mixture of DCM/MeOH (1 mL total volume) for 45 h at 27 °C. These specific conditions were chosen since they mimic the resin extraction procedure of the initial fermentation broth. LC-MS analysis of this reaction mixture showed the gradual appearance and growth of peaks that had identical retention times and mass fragmentations as **5** and **6**. Presumably, these compounds are produced by initial methanolysis of **1** to form **5** and then subsequent intramolecular nucleophilic displacement of the chloride by the adjacent hydroxyl group to form **6** (Figure 5).

The finding that **5** and **6** could be produced from **1** called into question the origin of compounds **7**–**9**. It was possible that **7**–**9** were produced from **1** through a decarboxylation mechanism. There is ample precedence for the decarboxylation of β-lactones, but this reaction usually requires elevated temperatures in excess of those experienced by **1** during the isolation process.[23] To explore this possibility a sample of **1** (1 mg) was stirred at 27 °C in a solution of 0.5 M NaOH, which had been buffered to pH 8 with HCl, and acetonitrile (0.5 mL each of the CH$_3$-CN and NaOH). This was the same pH as the fermentation broth initially. Aliquots of this mixture, which were analyzed by LC-MS over the course of 17 h, showed that **1** was being converted into a suite of related compounds during this time period, as shown by the UV chromatograms of the reaction mixture monitored at 210 and 254 nm. Compounds **7**–**9** could be clearly identified in the reaction mixture on the basis of comparison of the retention times and the corresponding molecular ions with those of the samples of **7**–**9** that had been characterized spectroscopically. Co-injection of authentic samples of **7**–**9** provided further proof for the degradation of **1** into these compounds. Given these overall observations, it was clear that compounds **5**–**9** were produced during the isolation process and are not natural products (Figure 5). It should be noted that the conversion of **1** into **5**–**9** established the absolute configurations of all these products since the configuration of C-6 is preserved as *S*.[24]

The finding that **7**–**9** can be formed from **1** necessitates a few comments. Conceptually, there are two general pathways for the conversion of **1** into **7**–**9**. The most important difference, as it relates to the following discussion, between the two possible pathways is that in route A the *S* absolute configuration of **1** at C-5 *is* retained in the products **8** and **9**, while in route B the absolute configuration of **1** at C-5 *is not* retained in the products **8** and **9**. While the exact mechanistic details of this conversion are not important for the following discussion, one possible mechanism for each route will still be discussed to illustrate this point about the different stereochemical outcomes. One hypothetical route A reaction pathway involves, after saponification, decarboxylation of the resulting vinylogous-δ-amide acid[25] to produce an aromatic pyran ring. Subsequent tautomerization of **13** produces a mixture of two diastereomers that are epimeric at C-4 (**8** and **9**) but that retain the *S* configuration at C-5 (Figure 6, route A). Dehydration of these compounds **8** and **9** then produces **7**. By comparison, route B (Figure 6) might proceed through a concerted mechanism involving a decarboxylation/dehydration sequence that initially gives rise to **7** in which the 5*S* configuration of **1** is lost. Nucleophilic addition of water to **7** would then give rise to a mixture of diastereomers (**8** and **9**). The most important consequence of this pathway is that theoretically four diastereomers[26] should be produced by any route B reaction pathway. The

(21) Casiraghi, G.; Spanu, P.; Rassu, G.; Pinna, L.; Ulgheri, F. *J. Org. Chem.* **1994**, *59*, 2906–2909.

(22) Schiehser, G. A.; White, J. D. *Tetrahedron Lett.* **1986**, *46*, 5587–5590.

(23) (a) Lowe, C.; Vederas, J. C. *Org. Prep. Proced. Int.* **1995**, *27*, 305–346. (b) Pommier, A.; Pons, J. M. *Synthesis* **1993**, *5*, 441–459.

(24) Attempts to determine the absolute configuration of C-5 in **8** and **9** by preparation of the MTPA derivatives resulted in elimination to form **7**.

(25) For an example of decarboxylation of a β-amide ester under basic conditions, see: Shehata, I. A.; Glennon, R. A. *J. Heterocycl. Chem.* **1987**, *24*, 1291–1295.
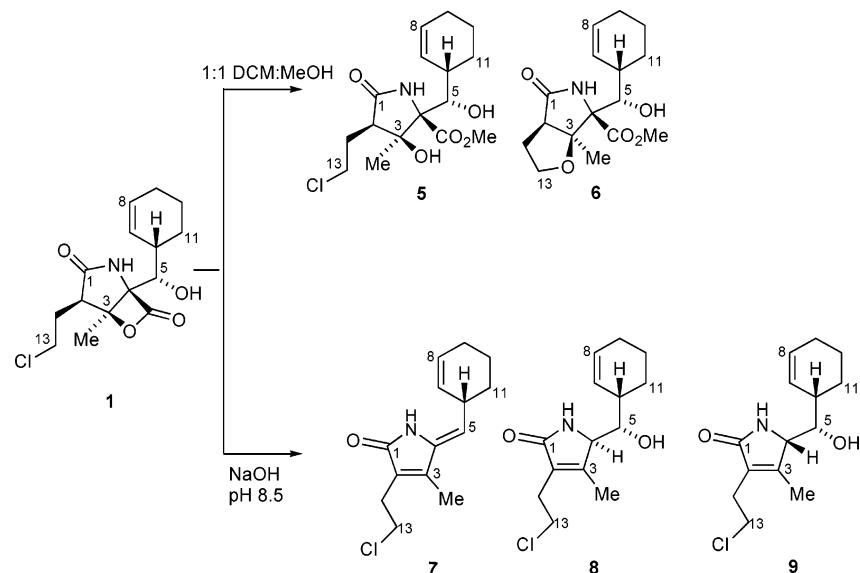
FIGURE 5. Reactivity of **1** toward MeOH and dilute NaOH.
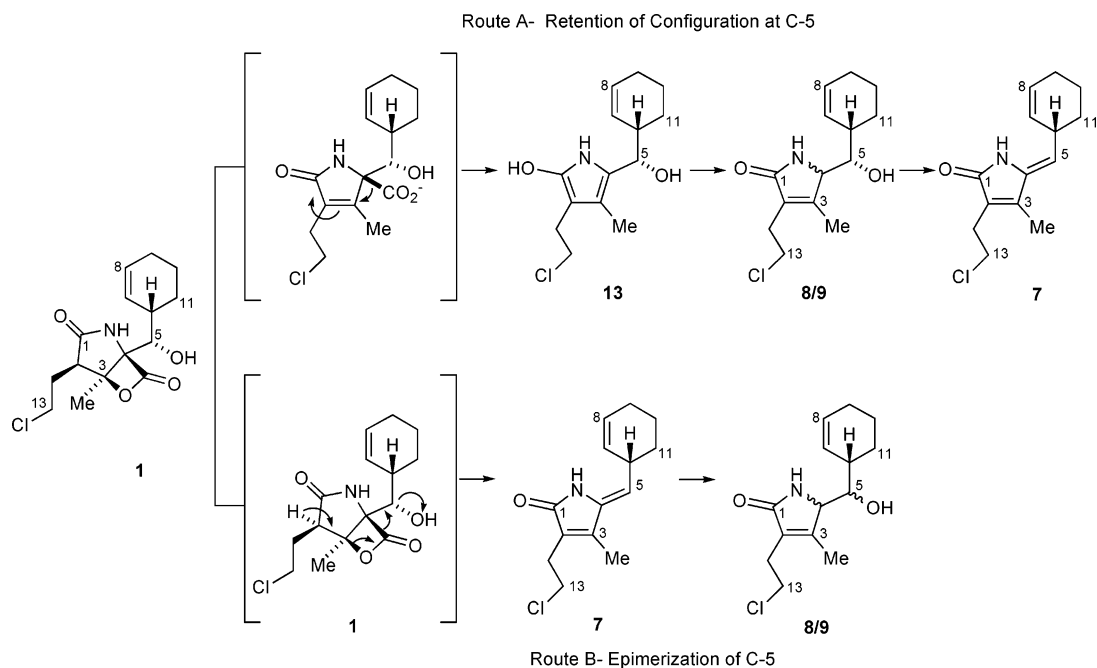
FIGURE 6. Possible degradation mechanisms.

isolation of just two diastereomers, **8** and **9**, from the fermentation mixture and, much more importantly, only those same two diastereomers from the degradation studies on **1** is evidence against the route B general mechanism. This evidence suggests that **8** and **9** are epimeric at C-4, as depicted, rather than at the alternative C-5 center. It should be noted that the above discussion also implies that **8** and **9** have an absolute configuration at C-5 of *S* analogous to salinosporamide A (**1**).

The finding that **5**−**9** can be produced from **1** also calls into question the origin of salinosporamide C (**4**). Clearly, on the basis of a number of factors, **4** is not a direct degradation product of salinosporamide A (**1**). Any "degradation" of **1** into **4** would require a number of transformations that would include decarboxylation of the β-lactone, oxidation of C-9 to a ketone, and formation of the pyrrole ring by the attachment of the nitrogen to C-7. This complexity makes it highly unlikely that **4** is a degradation product of salinosporamide A (**1**), but nevertheless it is still possible that **4** is an artifact caused by decarboxylation of the β-lactone compound **14** (Figure 7). A detailed analysis of the culture broth by LC-MS over the duration of the fermentation has not led to the identification of this putative metabolite; thus, we must

(26) Molecular modeling of the four potential diastereomers (4*R*,5*R*,6*S*; 4*R*,5*S*,6*S*; 4*S*,4*R*,6*S*; 4*R*,5*R*,6*S*) indicates that the lowest energy conformers of these diastereomers are all within 2 kcal/mol. This suggests that all four diastereomers should be produced, albeit in unequal amounts.
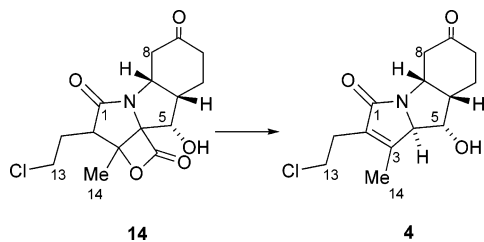
FIGURE 7. Hypothetical precursor of **4**.

TABLE 3. GI$_{50}$ Values for 1 and 3−9 (Values in μM)

compd[a]	HCT-116[a]	mean GI$_{50}$[b]	LOC-IMVI[c]	HOP-92[d]	OVCAR-3[e]	PC-3[f]
1	0.035	<0.011	<0.011	<0.011	<0.011	<0.011
3	20	NT[g]	NT	NT	NT	NT
4	>275[h]	NT	NT	NT	NT	NT
5	>225[h]	68	>100	>100	>100	>100
6	>151[h]	69	>100	<0.010	>100	0.174
7	>310[h]	58	54	18	no value given	44
8	139	83	>100	>100	3.7	>100
9	31	NT	NT	NT	NT	NT

[a] Human colon carcinoma. [b] Against the NCI 60-cell-line panel. [c] Melanoma. [d] Non-small lung cancer. [e] Ovarian cancer. [f] Prostate cancer. [g] Not tested against this cell line due to insufficient material. [h] These values all correspond to an upper limit in the assay of 78 μg/mL.

still consider **4** a natural product. The parent ring structure of **4** has been found in other natural products, although this exact oxidation pattern has not been observed. The closest structural relative of **4** would be the mitomycin family of antitumor antibiotics, which are distinguished by their ability to cross-link the complementary strands of DNA.[27]

The biological activities of all the isolated compounds were evaluated against several cancer cell lines. When tested against the human colon carcinoma HCT-116, compounds **1**, **3**, **8**, and **9** all inhibited growth (Table 3); salinosporamide A (**1**) was the most potent cytotoxin by more than 2 orders of magnitude, while compounds that lacked the β-lactone moiety, in general, displayed no significant cytotoxicity. This trend was consistent with the SAR data for omuralide (**2**), which proved that the β-lactone moiety was the key pharmacophore in that compound.[28] Several of these isolated compounds were also evaluated against the oncologically diverse 60-cell-line panel at the National Cancer Institute.[29] The GI$_{50}$ values for **5−8** varied significantly.[30] Compound **7** had only a weak inhibitory effect on the 60-cell panel with a mean GI$_{50}$ of 58 μM. The methyl ester **5** had no appreciable effect on any of the cancer cell lines. The tetrahydrofuran derivative **6** had a GI$_{50}$ of less than 10 nM against the non-small-cell lung cancer HOP-92 and a GI$_{50}$ of 174 nM against the prostate cancer PC-3, while **8** had a GI$_{50}$ of 3.7 μM against the ovarian cancer

(27) Pas, M. M.; Das, A.; Palom, Y.; He, Q. Y.; Tomasz, M. *J. Med. Chem.* **2001**, *44*, 2834−2842.

(28) (a) Fenteany, G.; Standaert, R. F.; Lane, W. S.; Choi, S.; Corey, E. J.; Schreiber, S. L. *Science* **1995**, *268*, 726−731. (b) Corey, E. J.; Li, W.-D. Z. *Chem. Pharm. Bull.* **1999**, *47*, 1−10. (c) Masse, C. E.; Morgan, A. J.; Adams, J.; Panek, J. S. *Eur. J. Org. Chem.* **2000**, *14*, 2513−2528.

(29) Boyd, M. R.; Paull, K. D. *Drug. Dev. Res.* **1995**, *34*, 91−109.

(30) Concentration that limited the growth of a cell line to 50% of the untreated control growth.

TABLE 4. LC$_{50}$ of 1 against Selected Cancer Cell Lines

cancer cell line type	cell line	LC$_{50}$ (μM)
non-small cell lung cancer	NCI−H226	<0.011
	NCI−H522	0.043
colon cancer	HCC-2998	0.018
CNS cancer	SNB-75	<0.011
melanoma	SK-MEL-28	<0.011
	SNB-75	0.032
renal cancer	A498	0.011
	RXF 393	0.023
breast cancer	MDA-MB-435	<0.011
leukemia	CCRF-CEM	>100
prostate cancer	DU-145	>100

OVCAR-3. By comparison, the GI$_{50}$ values for salinosporamide A (**1**) were less than 11 nM against all the cell lines in the panel. Further evaluation revealed that **1** was remarkably potent, with LC$_{50}$ values[31] of less than 11 nM against certain non-small-cell lung, CNS, and breast cancer cell lines (Table 4; see Supporting Information Table S7 and S8 for complete results), and had low nanomolar activity against several other cancer cell lines. Salinosporamide A was remarkably selective against the panel of CNS and renal cancers, with a difference of over 3 orders of magnitude between the LC$_{50}$ values for the two most sensitive cell lines in each of those categories. This selectivity was further expressed by the lack of any significant toxicity (LC$_{50}$) against any of the leukemia and prostate cancers (>100 μM) despite its impressive activity against the other cell lines.

Salinosporamide A (**1**) has been shown to be 35 times more potent than omuralide (**2**) in inhibiting the chymotrypsin-like activity of the 20S subunit.[8] This finding was intriguing since the extensive SAR data on omuralide (**2**) suggested that salinosporamide A (**1**) should be less active due to the increased steric bulk of the substituents on C-2 and C-6.[17] The discovery of **3**, the deschloro-analogue, may shed some light on this discrepancy, as **3** was approximately 500 times less cytotoxic against HCT-116 when compared to **1** (**3**, GI$_{50}$ = 20 μM; **1** GI$_{50}$ = 0.035 μM). In fact, **3** displayed approximately the same cytotoxicity as **9**, a compound that does not possess the β-lactone. Taken together, these data indicate that the β-lactone is the key pharmacophore, but they also suggest that the chloroethyl group is important for the cytotoxicity of **1**, as demonstrated by the difference in activity between **1** and **3**. Evaluation of the ability of **3** to inhibit the 20S subunit of the proteasome is underway and should shed some light on this important issue.[32] The data presented here also raise one question regarding the SAR data on omuralide. While there is no guarantee that the relative difference in the ability to inhibit the proteolytic activity of the proteasome should parallel the difference in cytotoxicity against HCT-116, the data presented here do raise the possibility that a chlorinated omuralide analogue would display a similarly large increase in potency as was seen between **1** and its deschloro analogue **3**.[33] As a final note, compounds **1** and

(31) Concentration that killed 50% of the treated cell line as compared to the untreated cells.

(32) For the results of this study, see: Macherla, V. R.; Mitchell, S. S.; Manam, R. R.; Reed, K. A.; Chao, T.-H.; Nicholson, B.; Deyanat-Yazdi, G.; Mai, B.; Jensen, P. R.; Fenical, W.; Neuteboom, S. T. C.; Lam, K. S.; Palladino, M. A.; Potts, B. C. M. *J. Med. Chem.* **2005**, *48*, 3684−3687.

3−9 were evaluated in a series of antimicrobial and antiviral assays. All compounds (**1**, **3−9**) did not inhibit the growth of antibiotic-resistant strains of *Staphylococcus aureus* (methicillin-resistant), *Enterococcus faecium* (vancomycin-resistant), and *Candida albicans* (wild-type and amphotericin-resistant) and *Herpes simplex* virus.[34]

The observed chemical stability of **1** provides insight that should help define the guidelines for the formulation and possible routes of administration of the salinosporamides as they enter phase 1 clinical trials. Likewise, the SAR data gained from the isolation and extensive testing of **1** and **3−9** have confirmed the β-lactone as the crucial pharmacophore of the salinosporamides but raise intriguing questions about the role of the chloroethyl moiety in influencing the biological activity. The evidence seems to suggest that the chloroethyl unit in salinosporamide A (**1**) is the reason that the SAR conclusions about the effect of bulky substituents at C-2 and C-5 in omuralide[17] do not seem to apply to **1**.

---

(33) Recent results suggest that this might indeed be the case. Reddy, L. R.; Fournier, J.-F.; Reddy, B. V. S.; Corey, E. J. *J. Am. Chem. Soc.* **2005**, 7, 2699−2701

(34) Upper limit on the antibacterial, antifungal, and antiviral assays is 250, 500, and 20 μg/mL, respectively.

Supporting Information Available: General experimental procedures and characterization of **3−9**; tabulated NMR data for **5−9**; ^{1}H and ^{13}C NMR spectra for **3−9**; two-dimensional NMR spectra for **3**, **4**, **6**, **8**, and **9**; and results for **1** against NCI's 60-cell-line panel. This material is available free of charge via the Internet at http://pubs.acs.org.

JO050511+